nature reviews molecular cell biology

https://doi.org/10.1038/s41580-025-00843-2

Supplementary information

Recommendations for robust and reproducible research on ferroptosis

In the format provided by the authors and unedited

<u>Supplementary Figure 1:</u> Isoforms of GPX4, SLC7A11, FSP1 and ACSL4

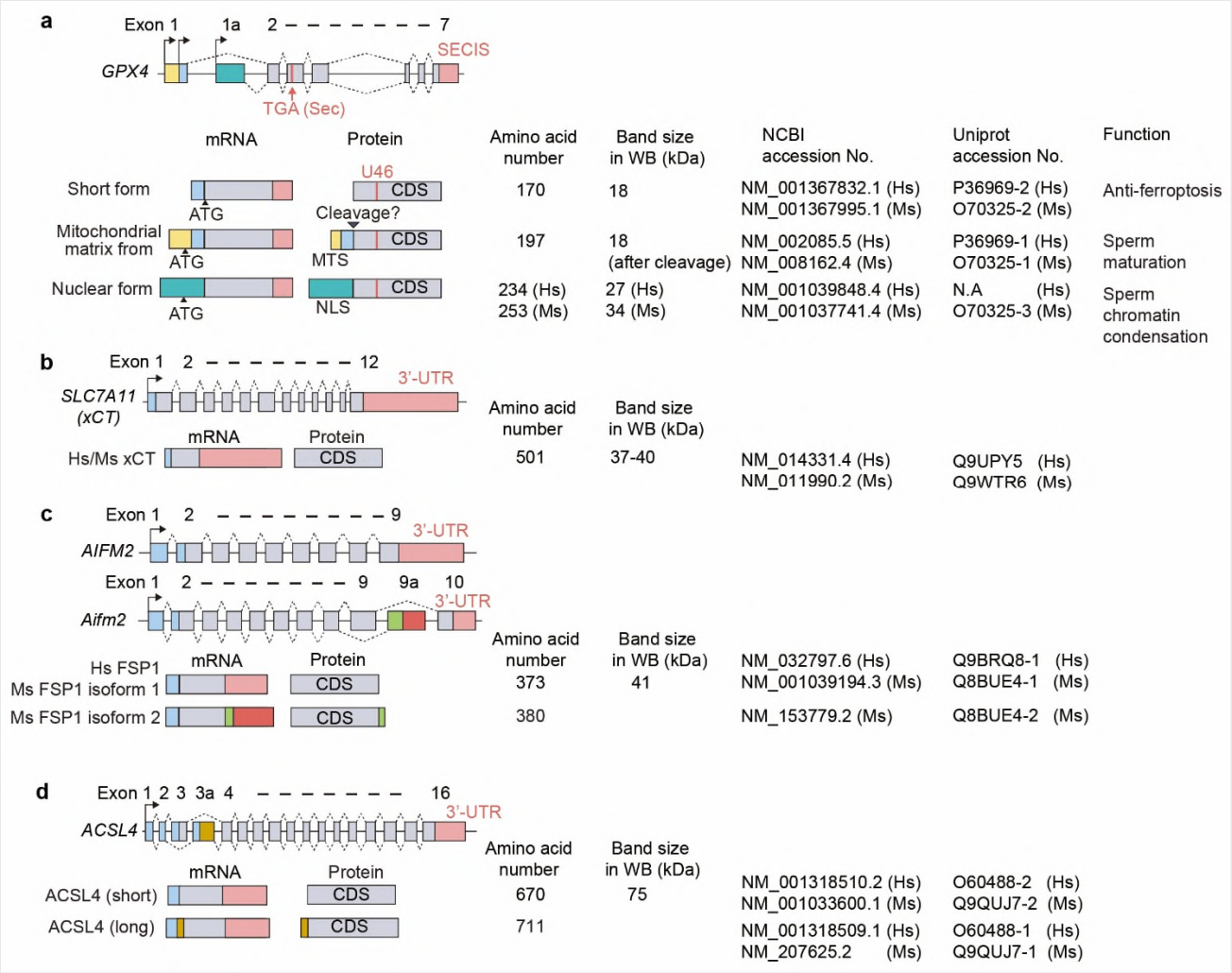

a. *GPX4* in humans (Hs) and mice (Ms) consists of 8 exons and encodes for 3 isoforms. To decode the UGA codon for selenocysteine (Sec), the *GPX4* mRNA contains a selenocysteine insertion sequence (SECIS) element in the 3'-untranslated region (UTR, *red*). The short form, found in the cytosol, nucleus, nuclear membrane, plasma membrane and mitochondrial intermembrane space of somatic cells, protects against ferroptosis. The mitochondrial matrix form has an N-terminal mitochondrial targeting sequence (MTS, *yellow*) and is present in the mitochondrial matrix. The nuclear form, with an N-terminus encoded by an alternative exon (*green*), is the longest isoform. The mitochondrial matrix and nuclear forms are mainly expressed in the testis and play distinct roles in spermatogenesis.

b. Hs and Ms *SLC7A11/Slc7a11* is made up of 12 exons with long 3'-UTR. Although the predicted size of xCT is 55 kDa, the band of xCT is detected at approximately 35-40 kDa in Western blotting.

c. Hs *AIFM2* is made up of 9 exons. In Ms *Aifm2*, two isoforms are reported, in which one is encoded by 9 exons, and the other by 10 exons.

d. *ACSL4* has 2 different isoforms each made up of 16 exons.

<u>Supplementary Figure 2:</u> Functional assays of GPX4, FSP1, system x_c^- and ACSL4

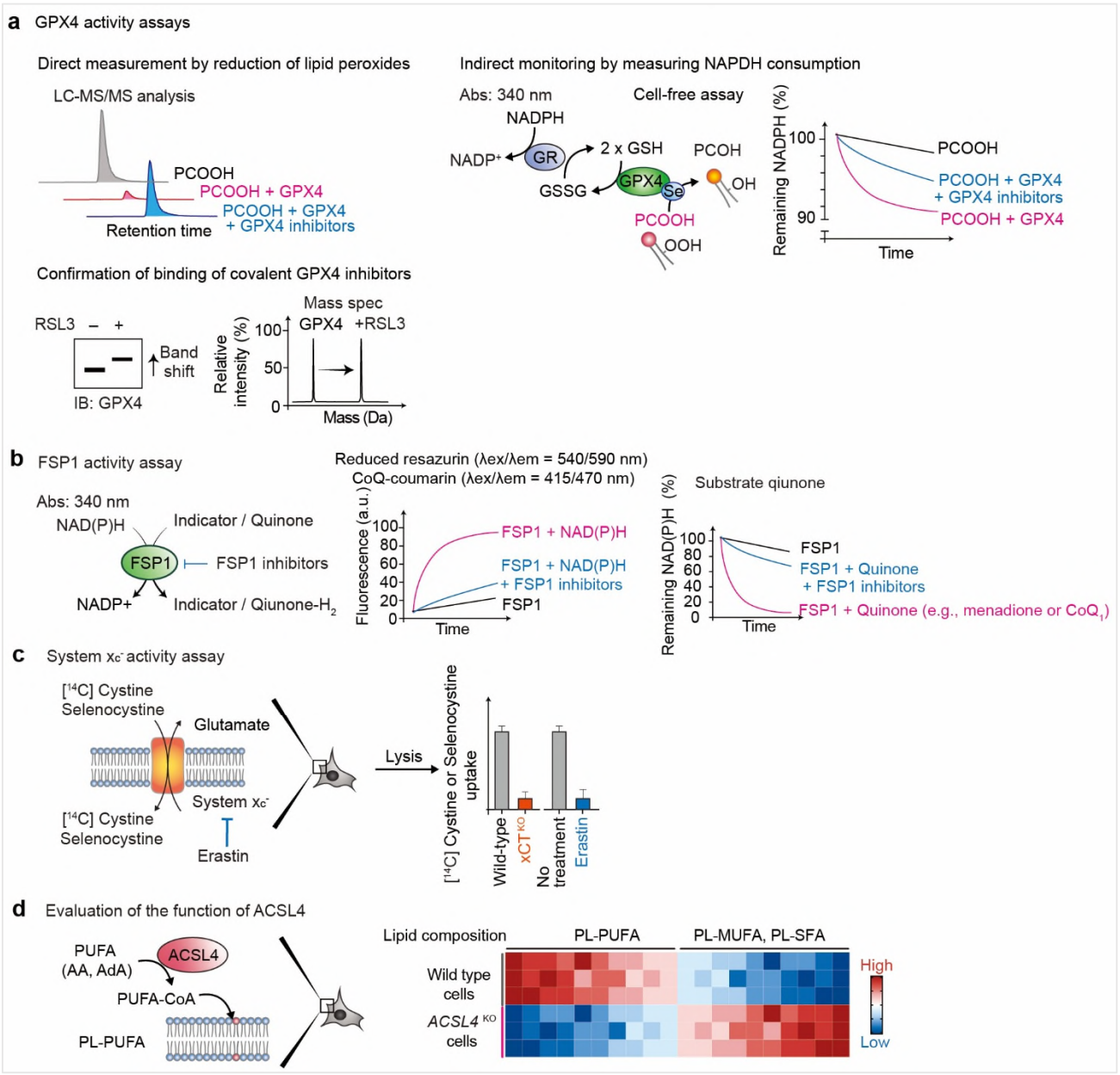

a. GPX4 activity can be determined by measuring the reduction of GSH-dependent lipid peroxides by mass-spectrometry, or indirectly monitored by measuring NADPH consumption, achieved by glutathione reductase (GR) coupled to the reduction of GSH upon reduction of substrate hydroperoxides by GPX4. As the substrates, purified phospholipid hydroperoxide (e.g., phosphatidylcholine hydroperoxide (PCOOH)) is recommended[1]. To evaluate the reactivity of a covalent GPX4 inhibitor towards GPX4, mass spectrometry analysis or immunoblotting analysis can be used. After treatment with the inhibitors, the band of GPX4 should shift slightly upward in immuno-blotting. In a-d, hypothetical graphs are shown as examples of the results.

b. To measure FSP1 enzymatic activity, NAD(P)H consumption or fluorescent substrates can be used with recombinant FSP1 protein[2,3]. FSP1 reduces resazurin or quinones using NAD(P)H; thus, FSP1 activity corresponds to the generation of the reduced form of resazurin or consumption of NAD(P)H.

c. To measure system x_c^- activity, an uptake assay using radioisotope-labeled ^{14}C cystine or selenocystine[4] as a substrate can be used.

d. To evaluate the effect of ACSL4, lipidomic analysis is used to measure the lipid composition, especially PUFAs/MUFAs ratio. AA, arachidonic acid; AdA, adrenic acid.

<u>Supplementary Table 1:</u> Available antibodies against GPX4, FSP1, xCT and ACSL4

Target	Host Species	Reactivity Species	Application	Working concentration	Validation by KO and OE cells	Identifier (Clone#)	Refs
GPX4	Rabbit, monoclonal	Hs, Ms	WB, IHC	1:1000 (WB), 1:100 (IHC)	KO & OE	Abcam, #ab125066	3
	Mouse, monoclonal	Hs, Ms	WB	1:1000 (WB)	OE	Proteintech, #67763-1-Ig	5
FSP1	Mouse, monoclonal	Hs	WB	1:1000 (WB)	KO & OE	SantaCruz, #sc-377120	3,6,7
	Rat, monoclonal	Hs	WB	1:1000 (WB)	KO & OE	Sigma Aldrich, #MABC1638 (6D8)	6,8
	Rat, Monoclonal	Hs, Ms	WB	1:100 (WB)	KO	Clone 1A1 (homemade) under commercialization	3,6
	Rat, Monoclonal	Hs, Ms	WB, ICC, IHC	1:1-5 (WB), 1:1 (ICC and IHC)	KO	Clone 14D7 (homemade) under commercialization	3,6
	Rabbit, Polyclonal	Ms	WB	Not described in the reference	OE	LS Bio, #LS-C382008	9
xCT	Rat, Monoclonal	Hs	WB, ICC (1*)	1:1000 (WB)	KO & OE	Abcam, #ab300667 (3A12)	8
	Rabbit, Polyclonal	Ms	WB, IHC (1*)	1:1000 (WB) 1:100 (IHC)	KO & OE	Cell Signaling, #98051	10
ACSL4	Mouse, monoclonal	Hs, Ms	WB only (*2)	1:200-1000 (WB)	KO & OE	SantaCruz #sc-271800	11,12
	Rabbit, Polyclonal	Hs	WB	1:2500 (WB)	KO	Sigma-Aldrich, #SAB2701949	13
	Rabbit, Polyclonal	Hs	WB only (*3)	1:1000 (WB)	KO & OE	GeneTex, #GTX100260	14,15
	Rabbit, Polyclonal	Hs, Ms	WB, ICC, IHC	1:1000 (WB, ICC) 1:500 (IHC)	KO & OE	Invitrogen, #PA5-27137	16,17
	Rabbit, monoclonal	Hs, Ms	WB	1:2000-5000 (WB)	KO	Abcam, #ab155282	12,18

*1: To detect xCT in WB, heat lysate samples in a sample buffer for 3 min at 50 ˚C (Do not boil). The detected band size of xCT should be around 35- 40 kDa.
*2: Lysates from cultured cells only; not recommended for tissues.
*3: Recognizes both ACSL3 and ACSL4.
KO, knockout; OE, overexpression; WB, Western blotting; IHC, immunohistochemistry; ICC, immunocytochemistry

<u>Supplementary Table 2:</u> Validated single guide RNA sequences against *GPX4, AIFM2, SLC7A11* and *ACSL4* for the generation of knockout cells by the CRISPR-Cas9 system

Target gene	Species	Targeted exon	Single guide RNA Sequence	Refs
GPX4	Human	3	CGTGTGCATCGTCACCAACG	[8]
GPX4	Human	3	CACGCCCGATACGCTGAGTG	[8,19]
GPX4	Human	1	AGCCCCGCCGCGATGAGCCT	[7]
GPX4	Human	2	CTTGGCGGAAAACTCGTGCA	[19]
Gpx4	Mouse	3	CGTGTGCATCGTCACCAACG	[3]
Gpx4	Mouse	3	CATGCCCGATATGCTGAGTG	[3]
AIFM2	Human	2	TCCCGATTCCACCGAGACCT	[6,7]
AIFM2	Human	7	GGTGCAGAGAATCACCAGGT	[6]
Aifm2	Mouse	2	GCCCACGATCACCACGTGCA	[3]
Aifm2	Mouse	2	GCCGTGCACGTGGTGATCGT	[3]
SLC7A11	Human	2	AAGTATTACGCGGTTGCCAC	[20]
SLC7A11	Human	1	GTGTTCTGGAGCACGCCCTT	[20]
Slc7a11	Mouse	1	ATCGGCACCGTCATCGGATC	[21]
Slc7a11	Mouse	1	ATCATCATCGGCACCGTCAT	[21]
ACSL4	Human	4	TGCAATCATCCATTCGGCCC	[7,13]
ACSL4	Human	4	TGGTAGTGGACTCACTGCAC	[7]
Acsl4	Mouse	3	ACAGAGCGATATGGACTTCC	[11]

<u>Supplementary table 3:</u> Reported mouse strains genetically engineered for *Gpx4, Aifm2, Slc7a11* or *Acsl4*

Allele symbol	Category	Description	Phenotype	References
Gpx4^{tm1Prol}	KO of all *Gpx4* isoforms; targeted (null/knockout)	Deletion of exons 3–7 of *Gpx4*.	Embryonic lethality, displaying abnormalities before E7.5.	Yant et al 2003[22]
Gpx4^{tm1Yana}	KO of all *Gpx4* isoforms; targeted (null/knockout)	Full deletion of all exons of *Gpx4*.	Early embryonic lethality.	Imai H et al 2003[23]
Gpx4^{tm1Ssd}	KO of all *Gpx4* isoforms; Targeted (null/knockout)	Part of exon 1 through part of exon 2 was replaced with a lacZ reporter gene and a neo cassette.	Early embryonic lethality.	Garry MR et al 2008[24]
Gpx4^{tm1Marc}	KO of nuclear form of *Gpx4*; targeted (null/knockout)	Deletion of the nuclear isoform of *Gpx4* by insertion of an EGFP-stop cassette into the alternative exon (1b).	Fertile and viable; abnormal sperm chromatin condensation when isolated from the caput epididymis.	Conrad et al 2005[25]
Gpx4^{tm3Marc}	KO of mitochondrial form of *Gpx4;* targeted (modified isoform(s))	Insertion of an in-frame translational STOP codon into exon (1a), 25 bp downstream of the mitochondrial *Gpx4* start codon.	Male infertility; severe structural sperm abnormalities reminiscent to rodents kept under prolonged selenium deficiency.	Schneider et al 2009[26]
Gpx4^{tm5Marc}	*Gpx4* U46S mutation in all *Gpx4* isoforms; targeted	Selenocysteine (U46) is replaced with a catalytically inactive serine (S) residue.	Embryonic lethality at E7.5–E8.5; male subfertility of heterozygous males of catalytically inactive GPX4, with a dominant-negative role in male fertility.	Ingold et al 2015[27]
Gpx4^{tm4Marc}	*Gpx4* U46C mutation in all *Gpx4* isoforms; targeted	Selenocysteine (U46) is replaced with a catalytically inactive Cysteine (C) residue.	On a mixed C57BL/6J x 129S6SvEv background, homozygous animals are born normally but lose body weight at P14-16 and need to be sacrificed due to severe epileptic seizures; reactive astrogliosis and microglia activation at parvalbumin-positive GABAergic interneurons. On a C57BL/6J background, homozygous animals die during embryogenesis E11.5 - E12.5.	Ingold et al 2018[28]
Gpx4^{tm2Marc} *(Gpx4*$^{fl/fl}$*)*	*Gpx4* flox; targeted conditional-ready null allele (CKO)	Exons 5–7 including the Sec-insertion sequence element and the polyadenylation signal were flanked by loxP sites.	Early embryonic lethality by homozygous *GPx4* deleted alleles.	Seiler et al 2008[29]
Gpx4$^{tm1.1Qra}$ *(Gpx4*$^{fl/fl}$*)*	*Gpx4* flox; targeted conditional-ready null allele (CKO)	A loxP site and FRT flanked neo cassette were inserted upstream of exon 2, and a loxP site was inserted downstream of exon 4 via homologous recombination.	Tamoxifen-treated Gpx4 f/f; cre mice lose body weight and die within 2 weeks.	Yoo SE et al. 2012[30]
Rosa26-CreERT2; Gpx4 $^{fl/fl}$	Conditional knockout of *Gpx4*	Exons 5–7 of *Gpx4* are deleted in the whole body (except brain) of mice (depending on R26-CreERT2 expression) after tamoxifen injection.	Mice develop acute kidney failure between 9-13 days after tamoxifen injection.	Friedmann Angeli et al 2014[31]
CamKIIα-Cre; Gpx4$^{fl/fl}$	Conditional knockout of *Gpx4*	Exons 5–7 of *Gpx4* are deleted in CamKII-expressing neurons (forebrain).	Ataxia and severe epileptic seizures shortly after birth; neurodegeneration in hippocampus and cortex of newborn mice.	Seiler et al 2008[29]
Alb-Cre; Gpx4$^{fl/fl}$	Conditional knockout of *Gpx4*	Exons 5–7 of *Gpx4* are deleted in hepatocytes.	Hepatocyte-specific *Gpx4*$^{-/-}$ mice die shortly after birth and present extensive hepatocyte degeneration; *Gpx4*$^{-/-}$ pups born from mothers fed a vitamin E-enriched diet survive	Carlson et al 2016[32]
Alb-CreERT2; Gpx4$^{fl/fl}$	Conditional knockout of *Gpx4*	Exons 5–7 of *Gpx4* are deleted in hepatocytes after tamoxifen injection.	Acute liver failure leading to the early lethality when vitamin E is deprived from the chow.	Mishima et al 2022[3]
Cdh5(PAC)-CreERT2; Gpx4$^{fl/fl}$	Conditional knockout of *Gpx4*	Exons 5–7 of *Gpx4* are deleted in vascular endothelial cells after tamoxifen injection.	Feeding a vitamin E-depleted diet results in paralysis and death of mice due to endothelial cell death and multiple infarctions.	Wortmann et al 2013[33]

Slc6a3-CreERT2; Gpx4$^{fl/fl}$	Conditional knockout of *Gpx4*	Exons 5–7 of *Gpx4* are deleted in dopaminergic neurons after tamoxifen injection.	Increased anxiety compared to control animals; the phenotype is further aggravated when combined with *Dj-1* KO.	Schriever et al 2017[34]
CamKIIα-CreERT2; Gpx4$^{fl/fl}$ (BIKO)	Conditional knockout of *Gpx4*	Exons 5–7 of *Gpx4* are deleted in the CamKII expressing neurons (forebrain) after tamoxifen injection.	Neurodegeneration in the hippocampus and cortex; spatial learning, memory and cognitive impairment.	Hambright et al 2017[35]
Tg(Thy1-cre/ERT2,-EYFP)HGfng/PyngJ; Gpx4$^{fl/fl}$	Conditional knockout of *Gpx4* with simultaneous EYFP expression	Exons 2–4 of *Gpx4* are deleted in the majority of projection neuron populations in the central and peripheral nervous system after tamoxifen injection. The same neuronal population expresses enhanced yellow fluorescent protein to allow cell tracking.	Rapid motor neuron degeneration and paralysis.	Chen et al 2015[36]
Pax8rtTA-tetO-Cre; Gpx4$^{fl/fl}$	Doxycycline inducible knockout of *Gpx4* in renal tubular epithelial cells	Doxycycline feeding induces Cre-mediated deletion of exons 2–4 of *Gpx4* in renal tubular epithelial cells.	Tubular injury and reduced kidney function; the observed phenotypes in males are more severe than in females.	Ide et al 2022[37]
CD4-Cre; Gpx4$^{fl/fl}$	Targeted (null/knockout); all *Gpx4* isoforms	Exons 5–7 of *Gpx4* are deleted during T cell development in lymphoid tissues.	Loss of *Gpx4* results in an intrinsic T cell developmental defect in the periphery, which leads to a failure to expand and protect against acute viral and parasitic infections; dietary vitamin E supplementation can restore viability.	Matsushita et al 2015[38]
Tg(loxP-mGpx4KO); Gpx4$^{-/-}$	Targeted (null/knockout); mitochondrial *Gpx4*	Exons 3–7 of *Gpx4* are deleted; endogenous *Gpx4* expression of all isoforms is replaced by a *Gpx4* transgene carrying loxP sites before exon 2 and after exon 7 and missing the mitochondrial start codon. Expression of the *Gpx4* transgene is driven by 5' and 3' UTR regions of the endogenous *Gpx4* locus.	Cone–rod dystrophy-like phenotype in which loss of cone photoreceptors precedes loss of the rod photoreceptors.	Azuma et al 2022[39]
Crx-Cre;Tg(loxP-Gpx4);Gpx4 $^{-/-}$	Targeted (null/knockout); all *Gpx4* isoforms	The cone-rod homeobox (*Crx*) specific promoter drives the expression of a Cre recombinase, which deletes exons 3-7 of *Gpx4*.	Rapid and massive retinal degeneration.	Ueta et al 2012[40]
Pgk2-Cre;Tg(loxP-Gpx4);Gpx4 $^{-/-}$	Targeted (null/knockout); all *Gpx4* isoforms x targeted conditional-ready null allele (CKO)	The *pgk-2* specific promoter drives the expression of a Cre recombinase which deletes exons 3–7 of *Gpx4*.	Spermatocyte-specific *Gpx4* KO; impaired fertility and abnormal epididymal spermatozoa.	Imai et al 2009[41]
Adipoq-Cre; Gpx4$^{fl/fl}$	Targeted (null/knockout) in adipocytes	Exons 2–4 of *Gpx4* are deleted during adipocyte differentiation; Adipose-tissue specific *Gpx4* KO.	Spontaneous metabolic dysregulation such as disturbed glucose metabolism, impaired glucose tolerance and increased insulin resistance and systemic low-grade inflammation.	Schwärzler et al 2022[42]
Fabp4-Cre; Gpx4$^{fl/wt}$	Targeted (null/knockout) in brown and white adipose tissue	Heterozygous deletion of exons 2–4 of *Gpx4* in brown and white adipose tissue driven by *Fabp4-Cre*.	Spontaneous metabolic dysregulation such as disturbed glucose metabolism, impaired glucose tolerance and increased insulin resistance and systemic low-grade inflammation.	Schwärzler et al 2022[42]
POMC-Cre; Gpx4$^{fl/fl}$	Targeted (null/knockout) in POMC expressing neurons	Exons 5–7 of *Gpx4* are deleted in hypothalamic proopiomelanocortin (POMC) expressing neurons residing in the arcuate nucleus in the hypothalamus.	*Gpx4* is dispensable for the maintenance of cellular health and function of POMC neurons, even in mice exposed to obesogenic conditions.	Schriever et al 2017[34]
AgRP-Cre; Gpx4$^{fl/fl}$	Targeted (null/knockout) in AgRP expressing neurons	Exons 5–7 of *Gpx4* are deleted in agouti-related protein (AgRP) expressing neurons residing in the arcuate nucleus in the hypothalamus.	Mice fed a high-fat high-sucrose diet display increased body adiposity compared to controls.	Schriever et al 2017[34]

Foxp3YFP-Cre; Gpx4$^{fl/fl}$	Targeted (null/knockout) in Foxp3 expressing T regulatory (Treg) cells	Exons 2–4 of *Gpx4* are deleted in Foxp3 expressing Treg cells.	*Gpx4* KO mice reduce tumor growth via activating anti-tumor immunity.	Xu et al 2021[43]
Tg(GPX4)	Transgenic insertion of human *GPX4* including flanking regions.	DNA containing an intact human *GPX4* gene (~3 kb) plus ~30 and 20 kb of 5′- and 3′-flanking sequences was injected into fertilized oocytes derived from B6D2F1 mice to generate the transgenic mouse line.	Liver damage and lipid peroxidation induced by diquat are reduced significantly in Tg(GPX4) mice; when crossed with a model of amyotrophic lateral sclerosis (ALS) lifespan is slightly increased. *GPX4* tg can rescue the *Gpx4* null background; additionally, the SOD1(G93) mutant is mildly rescued by *GPX4tg.*	Q Ran et al 2004[44]; Chen et al 2021[45]
Aifm2$^{-/-}$	Targeted (null/knockout); *Aifm2*	Part of exon 2 is replaced by a neo cassette.	*Aifm2$^{-/-}$* mice are fully viable and fertile.	Mei et al 2006[46]
Aifm2$^{-/-}$	Targeted (null/knockout); *Aifm2*	Exons 5 and 6 of *Aifm2* are replaced by a *lacZ-neo* cassette.	No antidotal effect of vitamin K against warfarin overdose; increased damage during kidney ischemia reperfusion injury.	Mishima et al 2022[3]; Tonnus et al 2021[47]
Aifm2$^{-/-}$	Targeted (null/knockout); *Aifm2*	Global *Aifm2$^{-/-}$* mice using the CRISPR/Cas9 system.	*Aifm2$^{-/-}$* mice have higher body weights; *Aifm2$^{-/-}$* mice cannot maintain body temperatures upon cold; *Aifm2$^{-/-}$* mice decreases thermogenesis and energy expenditure, resulting in higher adiposity.	Nguyen et al 2020[48]
UCP1-Cre;Tg(β-Actin-fl-stop-fl-Aifm2)	Conditional transgenic in brown and white adipose tissue	*Aifm2* flox mice were generated using CRISPR/Cas9 system and cross bread with UCP1-Cre mice to direct Cre expression in interscapular brown fat at room temperature, and in inguinal and epididymal white adipose tissue after cold exposure.	Lower body weight with smaller white adipose tissue mass without any differences in lean mass compared to WT mice; enhanced thermogenesis, resulting in decreased adiposity of transgenic mice.	Nguyen et al 2020[48]
Slc7A11$^{-/-}$	Targeted (null/knockout); *Slc7a11*	A part of exon 1 was replaced by a GFP-Neo cassette.	Healthy in appearance and fertile. *Slc7a11$^{-/-}$* mice contain higher concentrations of cystine and lower concentrations of glutathione in plasma. *Slc7a11$^{-/-}$* mice show more severe lung damage induced by paraquat.	Sato et al 2005[49] Kobayashi et al 2012[50]
Slc7A11$^{-/-}$	Targeted (null/knockout); *Slc7a11*	The CRISPR/Cas9 system was used to generate KO mice.	Tumor growth of MC38 cells in *Slc7a11* KO mice has no impact on tumor development.	Arensman et al 2019[21]
Slc7a11$^{-/-}$	Targeted (null/knockout); *Slc7a11*	The CRISPR/Cas9 system was used to generate KO mice by oocyte injection.	Melanoma development in *Slc7a11* KO mice was significantly slower than in *Slc7a11* control mice.	Chen et al 2023[45]
Slc7a11^{tm1a} (Slc7A11$^{fl/fl}$)	Targeted allele knockout	EUCOMM targeting vector was electroporated in ES cells and selected clones used in blastocysts injections.	Disruption of *Slc7a11* affect the intercellular communication in the suprachiasmatic nucleus.	Zhang et.al 2022[51]
Ella-Cre;Slc7A11$^{fl/fl}$	Targeted (null/knockout); *Slc7a11*	Exon 2 of *Slc7a11* is deleted in the early mouse embryo.	KO of *Slc7a11* aggravated Ang II-mediated mouse cardiac fibrosis, hypertrophy, and dysfunction.	Zhang et.al 2022[52]
Acsl4$^{-/+}$	Targeted (null/knockout); *Acsl4*	A part of exon 2 is replaced by a neo cassette.	Female mice heterozygous for *Acsl4* deficiency become pregnant less frequently and produce small litters.	Cho et al. 2001[53]
Acsl4^{tm1a} (Acsl4$^{fl/fl}$)	Targeted (null/knockout); *Acsl4*	EUCOMM targeting vector was electroporated into ES cells and selected clones used in blastocysts injections.	*Acsl4* KO mice attenuate paraquat and methotrexate-induced lung injury.	Tomitsuka et al 2023[54]
Adipoq-Cre; Acsl4$^{fl/fl}$	Targeted (null/knockout); *Acsl4*	Targeting vectors for exons 3–4 on the X chromosome was electroporated into ES cells to make loxP sites.	Adipocyte-specific *Acsl4* KO shows resistance to diet-induced obesity.	Killion et al; 2018[55]

Supplementary video: Live imaging of cells undergoing ferroptosis.

Pfa1 cells with inducible *Gpx4* deletion following treatment with 4-hydroxytamoxifen. The video was captured using Nanolive 3-D Cell Explorer 42-56 hours after the addition of 4-hydroxytamoxifen (1 μM). E. Mishima produced the video.

References:

1 Nakamura, T. *et al.* A tangible method to assess native ferroptosis suppressor activity. *Cell Rep Methods* **4**, 100710, doi:10.1016/j.crmeth.2024.100710 (2024).
2 Doll, S. *et al.* FSP1 is a glutathione-independent ferroptosis suppressor. *Nature* **575**, 693-698, doi:10.1038/s41586-019-1707-0 (2019).
3 Mishima, E. *et al.* A non-canonical vitamin K cycle is a potent ferroptosis suppressor. *Nature* **608**, 778-783, doi:10.1038/s41586-022-05022-3 (2022).
4 Shimomura, T. *et al.* Simple Fluorescence Assay for Cystine Uptake via the xCT in Cells Using Selenocystine and a Fluorescent Probe. *ACS Sens* **6**, 2125-2128, doi:10.1021/acssensors.1c00496 (2021).
5 Fang, J. *et al.* Overexpression of GPX4 attenuates cognitive dysfunction through inhibiting hippocampus ferroptosis and neuroinflammation after traumatic brain injury. *Free Radic Biol Med* **204**, 68-81, doi:10.1016/j.freeradbiomed.2023.04.014 (2023).
6 Nakamura, T. *et al.* Phase separation of FSP1 promotes ferroptosis. *Nature* **619**, 371-377, doi:10.1038/s41586-023-06255-6 (2023).
7 Bersuker, K. *et al.* The CoQ oxidoreductase FSP1 acts parallel to GPX4 to inhibit ferroptosis. *Nature* **575**, 688-692, doi:10.1038/s41586-019-1705-2 (2019).
8 Doll, S. *et al.* FSP1 is a glutathione-independent ferroptosis suppressor. *Nature* **575**, 693-698, doi:10.1038/s41586-019-1707-0 (2019).
9 Hendricks, J. M. *et al.* Identification of structurally diverse FSP1 inhibitors that sensitize cancer cells to ferroptosis. *Cell Chem Biol*, doi:10.1016/j.chembiol.2023.04.007 (2023).
10 Sprimont, L. *et al.* Cystine-glutamate antiporter deletion accelerates motor recovery and improves histological outcomes following spinal cord injury in mice. *Sci Rep* **11**, 12227, doi:10.1038/s41598-021-91698-y (2021).
11 Doll, S. *et al.* ACSL4 dictates ferroptosis sensitivity by shaping cellular lipid composition. *Nature Chemical Biology* **13**, 91-98, doi:10.1038/nchembio.2239 (2017).
12 Liao, P. *et al.* CD8(+) T cells and fatty acids orchestrate tumor ferroptosis and immunity via ACSL4. *Cancer Cell* **40**, 365-378 e366, doi:10.1016/j.ccell.2022.02.003 (2022).
13 Magtanong, L. *et al.* Exogenous Monounsaturated Fatty Acids Promote a Ferroptosis-Resistant Cell State. *Cell Chemical Biology* **26**, 420-432.e429, doi:10.1016/j.chembiol.2018.11.016 (2019).
14 Zhu, X. G. *et al.* CHP1 Regulates Compartmentalized Glycerolipid Synthesis by Activating GPAT4. *Mol Cell* **74**, 45-58 e47, doi:10.1016/j.molcel.2019.01.037 (2019).
15 Garcia-Bermudez, J. *et al.* Squalene accumulation in cholesterol auxotrophic lymphomas prevents oxidative cell death. *Nature* **567**, 118-122, doi:10.1038/s41586-019-0945-5 (2019).
16 Zheng, H., Jiang, L., Tsuduki, T., Conrad, M. & Toyokuni, S. Embryonal erythropoiesis and aging exploit ferroptosis. *Redox Biol* **48**, 102175, doi:10.1016/j.redox.2021.102175 (2021).
17 Li, Y. J. *et al.* Fatty acid oxidation protects cancer cells from apoptosis by increasing mitochondrial membrane lipids. *Cell Rep* **39**, 110870, doi:10.1016/j.celrep.2022.110870 (2022).
18 Wang, W. *et al.* CD8+ T cells regulate tumour ferroptosis during cancer immunotherapy. *Nature* **569**, 270-274, doi:10.1038/s41586-019-1170-y (2019).
19 Hangauer, M. J. *et al.* Drug-tolerant persister cancer cells are vulnerable to GPX4 inhibition. *Nature* **551**, 247-250, doi:10.1038/nature24297 (2017).

20 Yan, Y. *et al.* SLC7A11 expression level dictates differential responses to oxidative stress in cancer cells. *Nat Commun* **14**, 3673, doi:10.1038/s41467-023-39401-9 (2023).
21 Arensman, M. D. *et al.* Cystine–glutamate antiporter xCT deficiency suppresses tumor growth while preserving antitumor immunity. *Proceedings of the National Academy of Sciences of the United States of America* **116**, 9533-9542, doi:10.1073/pnas.1814932116 (2019).
22 Yant, L. J. *et al.* The selenoprotein GPX4 is essential for mouse development and protects from radiation and oxidative damage insults. *Free Radic Biol Med* **34**, 496-502, doi:10.1016/s0891-5849(02)01360-6 (2003).
23 Imai, H. *et al.* Early embryonic lethality caused by targeted disruption of the mouse PHGPx gene. *Biochem Biophys Res Commun* **305**, 278-286, doi:10.1016/s0006-291x(03)00734-4 (2003).
24 Garry, M. R. *et al.* Sensitivity of mouse lung fibroblasts heterozygous for GPx4 to oxidative stress. *Free Radic Biol Med* **44**, 1075-1087, doi:10.1016/j.freeradbiomed.2007.12.002 (2008).
25 Conrad, M. *et al.* The nuclear form of phospholipid hydroperoxide glutathione peroxidase is a protein thiol peroxidase contributing to sperm chromatin stability. *Mol Cell Biol* **25**, 7637-7644, doi:10.1128/MCB.25.17.7637-7644.2005 (2005).
26 Schneider, M. *et al.* Mitochondrial glutathione peroxidase 4 disruption causes male infertility. *FASEB J* **23**, 3233-3242, doi:10.1096/fj.09-132795 (2009).
27 Ingold, I. *et al.* Expression of a Catalytically Inactive Mutant Form of Glutathione Peroxidase 4 (Gpx4) Confers a Dominant-negative Effect in Male Fertility. *J Biol Chem* **290**, 14668-14678, doi:10.1074/jbc.M115.656363 (2015).
28 Ingold, I. *et al.* Selenium Utilization by GPX4 Is Required to Prevent Hydroperoxide-Induced Ferroptosis. *Cell* **172**, 409-422.e421, doi:10.1016/j.cell.2017.11.048 (2018).
29 Seiler, A. *et al.* Glutathione peroxidase 4 senses and translates oxidative stress into 12/15-lipoxygenase dependent- and AIF-mediated cell death. *Cell metabolism* **8**, 237-248, doi:10.1016/j.cmet.2008.07.005 (2008).
30 Yoo, S. E. *et al.* Gpx4 ablation in adult mice results in a lethal phenotype accompanied by neuronal loss in brain. *Free Radic Biol Med* **52**, 1820-1827, doi:10.1016/j.freeradbiomed.2012.02.043 (2012).
31 Friedmann Angeli, J. P. *et al.* Inactivation of the ferroptosis regulator Gpx4 triggers acute renal failure in mice. *Nature Cell Biology* **16**, 1180-1191, doi:10.1038/ncb3064 (2014).
32 Carlson, B. A. *et al.* Glutathione peroxidase 4 and vitamin E cooperatively prevent hepatocellular degeneration. *Redox Biol* **9**, 22-31, doi:10.1016/j.redox.2016.05.003 (2016).
33 Wortmann, M. *et al.* Combined deficiency in glutathione peroxidase 4 and vitamin E causes multiorgan thrombus formation and early death in mice. *Circ Res* **113**, 408-417, doi:10.1161/CIRCRESAHA.113.279984 (2013).
34 Schriever, S. C. *et al.* Alterations in neuronal control of body weight and anxiety behavior by glutathione peroxidase 4 deficiency. *Neuroscience* **357**, 241-254, doi:10.1016/j.neuroscience.2017.05.050 (2017).
35 Hambright, W. S., Fonseca, R. S., Chen, L., Na, R. & Ran, Q. Ablation of ferroptosis regulator glutathione peroxidase 4 in forebrain neurons promotes cognitive impairment and neurodegeneration. *Redox Biol* **12**, 8-17, doi:10.1016/j.redox.2017.01.021 (2017).
36 Chen, L., Hambright, W. S., Na, R. & Ran, Q. Ablation of the Ferroptosis Inhibitor Glutathione Peroxidase 4 in Neurons Results in Rapid Motor Neuron Degeneration and Paralysis. *J Biol Chem* **290**, 28097-28106, doi:10.1074/jbc.M115.680090 (2015).
37 Ide, S. *et al.* Sex differences in resilience to ferroptosis underlie sexual dimorphism in kidney injury and repair. *Cell Rep* **41**, 111610, doi:10.1016/j.celrep.2022.111610 (2022).
38 Matsushita, M. *et al.* T cell lipid peroxidation induces ferroptosis and prevents immunity to infection. *J Exp Med* **212**, 555-568, doi:10.1084/jem.20140857 (2015).
39 Azuma, K. *et al.* Mitochondrial glutathione peroxidase 4 is indispensable for photoreceptor development and survival in mice. *J Biol Chem* **298**, 101824, doi:10.1016/j.jbc.2022.101824 (2022).

40 Ueta, T. *et al.* Glutathione peroxidase 4 is required for maturation of photoreceptor cells. *J Biol Chem* **287**, 7675-7682, doi:10.1074/jbc.M111.335174 (2012).
41 Imai, H. *et al.* Depletion of selenoprotein GPx4 in spermatocytes causes male infertility in mice. *J Biol Chem* **284**, 32522-32532, doi:10.1074/jbc.M109.016139 (2009).
42 Schwarzler, J. *et al.* Adipocyte GPX4 protects against inflammation, hepatic insulin resistance and metabolic dysregulation. *Int J Obes (Lond)* **46**, 951-959, doi:10.1038/s41366-022-01064-9 (2022).
43 Xu, C. *et al.* The glutathione peroxidase Gpx4 prevents lipid peroxidation and ferroptosis to sustain Treg cell activation and suppression of antitumor immunity. *Cell Reports* **35**, 109235-109235, doi:10.1016/j.celrep.2021.109235 (2021).
44 Ran, Q. *et al.* Transgenic mice overexpressing glutathione peroxidase 4 are protected against oxidative stress-induced apoptosis. *J Biol Chem* **279**, 55137-55146, doi:10.1074/jbc.M410387200 (2004).
45 Chen, L. *et al.* Overexpression of ferroptosis defense enzyme Gpx4 retards motor neuron disease of SOD1G93A mice. *Sci Rep* **11**, 12890, doi:10.1038/s41598-021-92369-8 (2021).
46 Mei, J., Webb, S., Zhang, B. & Shu, H. B. The p53-inducible apoptotic protein AMID is not required for normal development and tumor suppression. *Oncogene* **25**, 849-856, doi:10.1038/sj.onc.1209121 (2006).
47 Tonnus, W. *et al.* Dysfunction of the key ferroptosis-surveilling systems hypersensitizes mice to tubular necrosis during acute kidney injury. *Nat Commun* **12**, 4402, doi:10.1038/s41467-021-24712-6 (2021).
48 Nguyen, H. P. *et al.* Aifm2, a NADH Oxidase, Supports Robust Glycolysis and Is Required for Cold- and Diet-Induced Thermogenesis. *Mol Cell* **77**, 600-617 e604, doi:10.1016/j.molcel.2019.12.002 (2020).
49 Sato, H. *et al.* Redox imbalance in cystine/glutamate transporter-deficient mice. *J Biol Chem* **280**, 37423-37429, doi:10.1074/jbc.M506439200 (2005).
50 Kobayashi, S. *et al.* Enhanced expression of cystine/glutamate transporter in the lung caused by the oxidative-stress-inducing agent paraquat. *Free Radic Biol Med* **53**, 2197-2203, doi:10.1016/j.freeradbiomed.2012.09.040 (2012).
51 Zhang, T. *et al.* High-throughput discovery of genetic determinants of circadian misalignment. *PLoS Genet* **16**, e1008577, doi:10.1371/journal.pgen.1008577 (2020).
52 Zhang, X. *et al.* SLC7A11/xCT Prevents Cardiac Hypertrophy by Inhibiting Ferroptosis. *Cardiovasc Drugs Ther* **36**, 437-447, doi:10.1007/s10557-021-07220-z (2022).
53 Cho, Y. Y. *et al.* Abnormal uterus with polycysts, accumulation of uterine prostaglandins, and reduced fertility in mice heterozygous for acyl-CoA synthetase 4 deficiency. *Biochem Biophys Res Commun* **284**, 993-997, doi:10.1006/bbrc.2001.5065 (2001).
54 Tomitsuka, Y. *et al.* Gene deletion of long-chain acyl-CoA synthetase 4 attenuates xenobiotic chemical-induced lung injury via the suppression of lipid peroxidation. *Redox Biol* **66**, 102850, doi:10.1016/j.redox.2023.102850 (2023).
55 Killion, E. A. *et al.* A role for long-chain acyl-CoA synthetase-4 (ACSL4) in diet-induced phospholipid remodeling and obesity-associated adipocyte dysfunction. *Mol Metab* **9**, 43-56, doi:10.1016/j.molmet.2018.01.012 (2018).